X-911-76-11

PREPRINT

NASA TM X- 71076

CHARACTERISTICS OF SOUTHERN HEMISPHERE 200 mb FLOW AS DETERMINED FROM SATELLITE DATA

(NASA-TM-X- 1076) CHARACTERISTICS OF SOUTHERN HEMISPHERE 200 mb FLOW AS DETERMINED FROM SATELIITE DATA (NASA) 27 p HC $4.00 CSCL 04A

N76-19651

Unclas G3/46 22156

ROBERT F. ADLER

JANUARY 1976

GSFC

GODDARD SPACE FLIGHT CENTER
GREENBELT, MARYLAND

Abstract

Characteristics of Southern Hemisphere 200 mb flow are examined using geopotential height fields constructed with the aid of satellite-based thermal structure. Similar Northern Hemisphere, satellite-based fields are developed in order to make inter-hemispheric comparisons. Results indicate that both the zonal and meridional components of the S.H. eddy kinetic energy are as large as their N.H. counterparts. In winter the principal inter-hemispheric difference with respect to eddy kinetic energy is that the S.H. standing eddies are much less important only to the meridional component. Zonal component standing energy is about equal in the two hemispheres. In summer the S.H. has larger zonal eddy kinetic energy than the N.H. and smaller standing eddy contributions in both components. Although transient eddies are generally predominant in the S.H., estimates in this study of the standing eddy contribution are larger than previous values. The meridional spectra show a preference for intermediate size ($k = 4, 5$) transient waves. Ratios of zonal to meridional energies indicate that, especially at intermediate wavelengths, the S.H. waves are "more meridional" than those in the N.H.

1. Introduction

The purpose of this paper is to describe certain characteristics of the large-scale, 200 mb flow in the Southern Hemisphere (S.H.) using geopotential height fields based on atmospheric temperature structure obtained from a satellite borne, multi-channel infrared radiometer. This study concentrates on the 200 mb level because it is a major contributor to the kinetic energy of the atmosphere and is representative of upper tropospheric or jet-stream flow patterns. Most previous studies of S.H. upper tropospheric flow have been based on data from the sparse radiosonde network there. Although estimates of parameters such as zonal-averaged zonal flow are fairly reliable, terms such as the kinetic energy contained in transient waves are difficult to describe adequately from the conventional data network. However, the satellite-based information used in this study has the spatial and temporal resolutions necessary to describe pertinent features of large-scale 200 mb flow.

This study uses one winter month and one summer month of daily analyses in both the S.H. and the Northern Hemisphere (N.H.). The N.H., satellite-based calculations are compared to calculations made with National Meteorological Center (NMC) gridded data. Therefore, the validity of conclusions based on the S.H., satellite-based calculations can be readily judged. The geostrophic approximation is used to obtain the winds from the geopotential height distributions.

The topics explored here include:

a. zonal flow

b. zonal and meridional eddy kinetic energy

c. standing and transient eddy contributions

d. spectral distribution of eddy kinetic energy

e. horizontal anisotropy

2. Method used to obtain geopotential height fields from SIRS radiances.

The satellite data for this study are from the Satellite Infrared Spectrometer (SIRS) instrument aboard the Nimbus 3 spacecraft. The technique used to obtain atmospheric structure information from the SIRS radiances is summarized by Adler (1975) and described in detail by Adler (1974). Basically, geopotential thickness or layer-mean temperature information is determined from the SIRS data by a linear regression technique. The dependent variables in the regression procedure are the thicknesses for the four following layers: 1000-700 mb, 700-500 mb, 500-300 mb and 300-200 mb. The independent variables are the radiances of the eight SIRS channels. Separate regression equations are determined for each layer and for each of the following latitude zones in both hemispheres: 20-40°, 40-60° and 60-80°.

The radiance data used is restricted to that portion determined to be "cloud-free" by an objective procedure based on the radiance data itself. Approximately 15% of the original data is eliminated as cloud-contaminated. The standard errors of estimate for the derived regression equations are comparable to those in other studies (e.g. Smith, Woolf and Jacob, 1970).

The geopotential height information at 200 mb is obtained by adding thicknesses to a 1000 mb height field. In the N.H., the NMC 1000 mb height fields are used. In the S.H., 1000 mb height analyses are obtained by converting daily surface pressure analyses of the Commonwealth Bureau of Meteorology, Australia. The S.H. surface pressure analyses are nearly hemispheric in scope, but where they are blank, the field is filled in subjectively by a combination of extrapolation and climatology.

The major limitation of the atmospheric structure obtained from the satellite radiances in this way is that longitudinal or east-west gradients tend to be underestimated. The reasons for this underestimation are discussed by Adler (1974, 1975). The effect is related to the distribution of satellite data and the tendency of the regression equations to produce accurate results near the mean thickness for a particular latitude band, but to undervalue deviations from that mean. The magnitude of the underestimation is evident in the N.H. comparisons between the conventional-based and satellite-based statistics. Because of this limitation, the emphasis here is not always on absolute magnitudes, but often on relative magnitudes (S.H. compared to N.H.).

3. Zonal and eddy kinetic energy

a. zonal flow

The standard notation for means and deviations will be used in the following discussions. Time and longitudinal averages will be denoted by an overbar and brackets, respectively, and deviations from these means are marked by a prime and asterisk, respectively. Therefore, $[\overline{u}]$ represents the time and longitudinal mean of the zonal flow.

Fig. 1 shows the distribution of the zonal mean geostrophic wind at 200 mb in the S.H. for July and January. The zonal mean winds as determined from the SIRS-based 200 mb heights are presented along with the climatology curves based on Taljaard et al. (1969). The two profiles for each month agree fairly closely, considering one is from a climatological distribution and the other is for a specific one month period. In winter (Fig. 1a), a secondary peak at 60S is evident in the SIRS profile, while the climatological curve shows only a very

weak relative maximum farther north. Since the SIRS curve is based on only one month of data, the existence of a secondary peak on a year-to-year basis is still very questionable. However, conventional data, upon which the climate curve is based, is very sparse in the 50-65S region. Therefore, that curve may also be open to question.

The existence or non-existence of the secondary maximum in $[\bar{u}]$ during winter has been discussed by Webster and Curtin (1974). Their data from the EOLE constant density balloon experiment does not show the second peak; however, the number of balloons aloft in midwinter was relatively small and the results during June, July, and August may not be representative. From climatological cross-sections especially at particular longitudes (see Van Loon, 1972), there appears to be a basis for a second peak of $[\bar{u}]$. The existence of the peak may depend heavily on the averaging period. Such a maximum may often exist on a monthly basis, but an average over a number of years of the same calendar month may reduce or remove the peak.

The zonal kinetic energy (KZ) calculated from $[\bar{u}]$ has already been discussed by Adler (1975). The most striking difference between the N.H. and S.H. is in the magnitude of KZ in the summer. At 200 mb the S. H., KZ is approximately three times as great as that in the N.H. This difference, of course, reflects the large difference in the $[\bar{u}]$ pattern in summer, with the peaks in the S.H. and N.H. being approximately 30 ms^{-1} and 20 ms^{-1}, respectively.

b. eddy kinetic energy

The eddy kinetic energy (KE) is defined, using the standard notation as:

$$KE = \frac{[\overline{u^{*2}}] + [\overline{v^{*2}}]}{2} \tag{1}$$

The standing and transient eddy portions of KE are given by:

$$KE(\text{standing}) = \frac{[\bar{u}^{*2}] + [\bar{v}^{*2}]}{2} \tag{2}$$

$$KE(\text{transient}) = \frac{[\overline{u'^2}] + [\overline{v'^2}]}{2} \tag{3}$$

In this case the time average is for a period of one month.

Some aspects of S.H. 200 mb eddy kinetic energy have already been examined by Adler (1975). The primary conclusion of that study was that at 200 mb the eddy kinetic energy (KE) is of about the same magnitude in both the N.H. and S.H., both in winter and summer. It was also shown that a smaller percentage of KE is contained in the standing eddies in the S.H. than in the N.H. The purpose of the present discussion is to examine the kinetic energy in terms of zonal and meridional components.

Tables 1 and 2 indicate the magnitudes of the mean 200 mb eddy kinetic energy associated with u and v components in the winter and summer. The values are area-weighted averages over the latitude band 20-80°. N.H. values computed from SIRS-based 200 mb height fields and from NMC height fields are presented for comparison with the S.H. values. A comparison of the N.H. NMC and SIRS columns makes it obvious that the energies are being underestimated by the SIRS-based calculations by approximately a factor of 2. However, the ratios of standing to total energy (rows 3 and 6) in the N.H. NMC and SIRS columns agree favorably. The reasons for the underestimation were mentioned in Section 2 and are discussed in detail by Adler (1974, 1975).

Table 1

Winter Zonal and Meridional Eddy Kinetic Energy

for Latitude Band 20-80°. Units $m^2\ s^{-2}$.

Winter	N.H.		S.H.
	January 1970 NMC	January 1970 SIRS	July 1969 SIRS
$\frac{u^2}{2}$ (standing)	37.8	18.6	18.0
$\frac{u^2}{2}$ (total)	90.7	50.2	51.5
ratio	0.42	0.37	0.35
$\frac{v^2}{2}$ (standing)	17.7	8.3	4.0
$\frac{v^2}{2}$ (total)	84.5	36.4	40.4
ratio	0.21	0.23	0.10

Table 2

Summer Zonal and Meridional Eddy Kinetic Energy

for Latitude Band 20-80°. Units: $m^2\ s^{-2}$.

Summer	N.H.		S.H.
	July 1969 NMC	July 1969 SIRS	January 1970 SIRS
$\frac{u^2}{2}$ (standing)	22.5	11.8	8.7
$\frac{u^2}{2}$ (total)	59.8	30.4	37.0
ratio	0.38	0.39	0.24
$\frac{v^2}{2}$ (standing)	11.2	5.3	3.4
$\frac{v^2}{2}$ (total)	54.3	24.9	28.4
ratio	0.21	0.21	0.12

The characteristics of the eddy kinetic energy in the S.H. as compared to the N.H. can be examined using the last two columns of Tables 1 and 2. These contain the satellite-based calculations in the two hemispheres. Although the SIRS-based values for the eddy energy are underestimates, the amount of underestimation should be approximately equal in the two hemispheres. Thus the N.H. and S.H. values can be examined to obtain relative magnitudes.

In winter (Table 1) the eddy kinetic energy of the zonal component ($u^2/2$) is approximately the same in the two hemispheres. This is true for both the standing and total energy and hence for the transient wave energy. However, the meridional component ($v^2/2$), in the lower half of Table 1, indicates a sharp difference between the hemispheres in the standing eddy energy and in the ratio of standing to total eddy energy. While the values of total eddy kinetic energy in the meridional component are about equal, the S.H. standing portion is one half that of the N.H. This results in a S.H. ratio of 0.10 compared to 0.23 for the N.H. The zonal component ratios are about the same above and below the equator. Therefore, in winter the principal difference between the hemispheres with respect to eddy kinetic energy is in the relative contributions of the standing and transient eddies to the meridional component of the eddy kinetic energy. The zonal component, on the other hand, has quite similar magnitudes in the two hemispheres with regard to both the standing and transient portions.

For the summer month (Table 2) the zonal eddy kinetic energy, $u^2/2$ (total), is larger in the S.H. than in the N.H. This is reasonable since the mean zonal flow $[\overline{u}]$ and the zonal kinetic energy are so much larger in the S.H. The term $v^2/2$ (total) is about the same in two hemispheres during this season. The S.H. standing-to-total ratio is smaller for both components in summer. As can be

seen from Tables 1 and 2, standing eddies contribute only half as much to the meridional eddy kinetic energy in the S.H. as they do in the N.H. The difference between the hemispheres in this regard for the zonal component is evident only in the summer.

Kao, Jenne, and Sagendorf (1970) present values of zonal and meridional eddy kinetic energy (both standing and transient) for various latitudes in the S.H. for the 500 mb level. Their study is based on conventional data from the International Geophysical Year (IGY). Based on their tabulated values, one can calculate the ratios of standing to total energy for both components at 500 mb. The result is substantially lower values for both components and for both seasons. Therefore, Kao et al indicate less energy in the S.H. standing eddies than does the present study. The earlier study, however, was based on the sparse S.H. radiosonde network of the IGY. The validity of the ratios in the current, satellite-based study is bolstered by the good agreement between conventional-based and satellite-based calculations in the N.H. Therefore, although the standing eddies in the S.H. are much weaker than in the N.H., they may be more significant than previously thought.

4. Spectral Characteristics

a. wave number spectra of u and v

The spectral coefficients are calculated from the daily 200 mb analyses and then averaged over the month to determine the mean spectra for the month. Spectra are also calculated from the monthly mean fields to determine the stationary eddy components. Because only a month of data goes into each spectrum, the results must be treated cautiously. For this reason, the spectra derived in this study are compared to previously derived spectra to ascertain

their representativeness. Unlike previous S.H. calculations, the current ones have the advantage of an immediate comparison with N.H. values calculated in an identical fashion from a very similar data base.

Figs. 2 and 3 display the wave number spectra for winter in both hemispheres for latitudes 30° and 50°, respectively. Fig. 4 shows the summer spectra for 50°. In winter latitude 30° is the approximate location of westerly wind maximum in both hemispheres, while in summer the maximum is located in the vicinity of 50°. In each diagram there are two N.H. curves: one based on calculations from the NMC gridded data, the other derived from the satellite-based atmospheric structure. The spectra are discrete and the lines connecting each calculated point at k = 1,2 . . . are merely to aid in displaying the distribution.

The N.H. spectra in Fig. 2 (winter, 30°) indicate that the underestimation of eddy amplitudes by the satellite-based information increases (percentage-wise) with increasing wave number k. However, the satellite-based spectra do show the same general characteristics as the conventional-based ones. For $u^2/2$, the N.H. has a peak at k = 1, a sharp drop-off of energy out to k = 3, and then a less rapid decrease. The S.H. spectrum also has its peak at k = 1, although wave number 2 does not contribute relatively as much at 30S as at 30N. The energy in $u_k^2/2$ (k = 1) at 30S is primarily in the stationary eddy (73%), while k = 2 has a much lower stationary contribution (26%). Beyond k = 3 the contribution is negligible. In the N. H., the wave numbers 1 and 2 have large (~ 70%) standing components and waves k = 3,4 also have significant (~ 25-40%) stationary contributions. The large amount of energy in standing wave number 1 in both hemispheres is due to the eccentricity of the polar vortex.

The spectra for the meridional component, v, at 30° (Fig. 2b) indicate the usual peaks at intermediate wavelengths. The agreement between the two N.H. curves is not good, although the positions of the absolute maxima are only one wave number apart. The S.H. spectrum shows a peak at k = 5, which agrees well with a peak in the 500 mb v spectra at k = 6 noted by Kao, Jenne and Sagendorf (1970) at 20S and 40S. The calculated percentage contribution of the standing eddies at k = 5 is 1%. The two surrounding wave numbers 4 and 6 have percentages of 20% and 11%, respectively. Therefore, the energy in the peak is almost completely associated with the transient waves. At similar wave numbers in the N.H., the standing eddy portion is larger (~20-30%).

Better agreement between the conventional and satellite-based calculations is evident in Fig. 3 for winter at 50° latitude. This closer agreement is related to the distribution of satellite data. The zonal spectra derived from both satellite and conventional data (Fig. 3a) have their peaks at k = 2 in the N.H. This disagrees with the N.H. mid-latitude spectra of Kao and Wendell (1970) at 200 mb, Kahn (1962) at 200 mb, and Saltzman and Fleisher (1962) at 500 mb, all of which have the zonal energy peak at k = 1. Benton and Kahn (1958), however, do show peak energy at k = 2,3 at 300 mb. Therefore, although both N.H. spectra have a zonal energy peak at k = 2 for January 1970, most other studies indicate the peak occurring at k = 1 in different years. The S.H. peak in Fig. 3a at k = 1 can be compared to Kao et al (1970) with peaks at k = 1 (40S) and k = 2 (60S), both at 500 mb. Since the energy in k = 1 is dependent on the eccentricity of the polar vortex, slight variations in vortex orientation will produce large changes in wave number 1 energy. Therefore, the wave number location of peak zonal energy is probably not a good parameter for inter-hemispheric comparison with such a

short time sample of data. However, it is obvious that the S.H. has a much more rapid decrease of zonal energy going toward higher wave numbers.

Approximately 35% of the energy in k = 2 (N.H.) is contributed by the stationary eddy. In the S.H., k = 2 has much less energy in the zonal component and essentially all that energy is in the transient portion. Wave number k = 1 in the S.H. is calculated to have an 81% stationary contribution.

The spectra of $v^2/2$ in Fig. 3b indicate perhaps the most striking disparity between the hemispheres. In the N.H. (50N) there are two peaks, at k = 2 and k = 6; at 50S there is one peak, at k = 4. At 50N the peak at k = 2 is predominently stationary wave energy (calculated values of 86% and 67% for the NMC and SIRS values, respectively), while at k = 6, the standing contribution is very small (< 10%). A double peak in v spectra at northern mid-latitudes is evident in most, but not all, previous studies. Saltzman (1958) indicates peaks at k = 3, 6 for one January at 500 mb. Benton and Kahn (1958) and Kahn (1962) display peaks at the same wave numbers for a two month winter period at 300 mb and 200 mb, respectively. One of these two months, however, coincides with Saltzman's January. Saltzman and Fleisher (1962) present tables indicating peaks at k = 3,5 for the cold six months of one year at 500 mb. However, the results of Kao and Wendell (1970) at 40N and 60N at 200 mb do not show double maxima, but have one peak at k = 5 at 40N and one peak at k = 3 at 60N. Therefore, although the double peak in the meridional spectrum is not in evidence in all studies, it is a common characteristic. The N.H. spectra of the present study can thus be considered representative. Also in agreement with the present investigation these previous studies have the stationary eddies dominating the energy in the low wave number peak, while the transient waves are the main contributors at the k = 5,6 peak.

At 50S the meridional spectra of the present study show maxima at k = 4 in both summer and winter. Wave number k = 5 has the second largest energy associated with it in both seasons. Therefore, wave numbers k = 4,5 appear to be the preferred wavelengths in the S.H. with wave number 4 having the maximum energy. The energy associated with these waves is almost entirely in the transient mode. Other S.H. investigations also exhibit spectral peaks in the same wave number region. Price (1975) displays S.H. spectra based on conventional data which have k = 4 as the dominant wave number. Kao, et al (1970), show peaks in the spectra at k = 6 (40S) and K = 5 (60S) in winter using geostrophic 500 mb winds calculated from the IGY data fields. Although their spectra do not have their absolute maxima at k = 4, the broader peaks of their study contain most of the energy in the wave numbers k = 4,5,6 (40S) and k = 3,4,5 (60S). In summer, peaks at k = 5 and k = 4 at 40S and 60S, respectively, are also noted by Kao et al (1970). Although previous S.H. studies are limited by the sparseness of the conventional data, they are still in good agreement with the results of the current study.

A summertime spectrum at 45S is also available from Desbois (1975). His spectrum is based on winds determined from tracking EOLE constant-level balloons at 200 mb. For the October 1971-February 1972 period, the meridional spectrum has a maximum at k = 5,6. Although this maximum is at slightly higher wave numbers, it is in general agreement with the spectra of the current study. Differences in these spectra are due to differences in the type of data, length of time interval used and natural variation.

The contrast in the N.H. and S.H. meridional spectra in Fig. 3b has possible implications with regard to the energy conversion process in the two hemispheres.

The winter-time conversion of eddy available potential energy to eddy kinetic energy in the N.H., when examined spectrally, has two peaks: at $k = 2$ and $k = 6$ (Saltzman and Fleisher, 1961; Wiin-Nielsen, 1959). The maximum at $k = 6$ is the larger of the two. These two peaks correspond to the maxima in the N.H. v spectra (Fig. 3b). This agreement merely reflects the association of poleward flow with ascent and equatorward flow with descent. Assuming the same relationships hold in the S.H. means that most of the energy conversion processes are occurring there on the scale of wave numbers 4-5. Thus the energy conversion processes in the S.H. are apparently carried out predominantly by transient eddies of a slightly larger size than their N.H. transient counterparts.

b. anisotropy

Wooldridge and Reiter (1970) indicate that significantly larger horizontal anisotropy at cyclone wavelengths exists in the S.H. compared to the N.H., with the v component being larger than the zonal component u. This conclusion is based on relative velocities of balloon pairs flown as part of the GHOST balloon program at 200 mb over the S.H. The calculated geostrophic winds of the present study offer a data set to examine this characteristic.

The ratio of u_k^2/v_k^2 was calculated and plotted as a function of k for latitude 50° in both hemispheres, for both winter and summer. The results are shown in Fig. 5. The two N.H. curves (conventional and satellite-based) are in good agreement. For $k \geq 3$, the S.H. distribution is quite a bit different from that in the N.H. in winter, and slightly different in summer. In winter, the ratio of u_k^2/v_k^2 is smaller in the S.H. for intermediate and shorter waves ($k \geq 4$). The difference is greatest at $k = 4,5$. These are the wave numbers of peak meridional

energy (see Fig. 3b). The summer distributions (Fig. 5b) show a smaller disparity and then only between wave numbers 3 and 5. At 30° latitude (diagram not shown here) in winter, the distinction shown in Fig. 5 does not occur. However, at mid-latitudes the S.H. does appear to have a tendency, especially in winter, to produce waves strongly anisotropic with the v component dominating the u component more than in the N.H. This confirms the observation of Wooldridge and Reiter (1970) and again indicates the intensity of meridional flow in S.H. eddies.

5. Conclusions

The flow at near-tropopause levels in the S.H. has significantly different characteristics than the comparable portion of the atmosphere north of the equator. This is apparent in the patterns of zonally-averaged flow, distributions of eddy kinetic energy, and in the spectral characteristics. The general picture of the S.H. upper tropospheric flow that is revealed is quite different from that of smooth zonal flow given by climatology.

In terms of the magnitude of the eddy kinetic energy, the eddies of the S.H. are as significant as those in the N.H. This is true for both the zonal and meridional components. However, the eddy kinetic energy of the two hemispheres does differ with regard to the relative contributions of standing and transient eddies. In general the S.H. is more highly dependent on transient eddies. This is especially true of the north-south component of the flow. As a result, time mean fields fail to show large eddies, particularly meridional eddies. Zonal eddy kinetic energy statistics are quite alike above and below the equator (Table 1). This is the case for both the standing and transient parts. With the meridional

eddy kinetic energy the story is much different. Although the total meridional eddy kinetic energy is nearly the same in the N.H. and S.H., the standing portion in the S.H. is only one half as large as that in the N.H. In summer (Table 2) the zonal eddy kinetic energy is larger in the S.H., although the meridional energy is about the same. Both components display smaller standing eddy contributions in the S.H. Although the standing eddies are less important in the S.H. than in the N.H., the present study shows evidence that they are greater contributors to the eddy kinetic energy than previously thought.

The meridional spectra for the S.H. indicate a preference for wave numbers $k = 4,5$. The energy at this wavelength is predominantly in the transient waves. In winter a single peak at $k = 4$ is noted at 50S, while at 50N peaks at $k = 2$ and $k = 6$ are evident. Because energy conversion processes are tied closely to north-south flow, S.H. energy conversions are probably carried out by intermediate sized transient waves, while in the N.H. large stationary and transient synoptic-scale ($k \sim 6$) waves are the principal converters.

Examination of 200 mb horizontal anisotropy as a function of wavenumber at latitude 50° reveals that the S.H. has a tendency to have the scale of meridional flow dominate over the zonal flow more than in the N.H. This feature is most evident in winter at $k \geq 4$. In summer it is restricted to $k = 3,4,5$. Therefore, the S.H. 200 mb flow at intermediate and shorter wavelengths appears to be influenced strongly by meridional motions, more so than even the N.H.

The zonally-averaged zonal flow patterns derived in the present study generally agree with S.H. climatology. The $[\overline{u}]$ pattern for July (winter) does, however, indicate a high latitude (60S-65S), secondary maximum which does not appear in some other published distributions.

REFERENCES

Adler, R. F., 1974: A comparison of the structure and flow characteristics of the upper troposphere and stratosphere of the Northern and Southern Hemispheres. Atmos. Sci. Paper No. 216, Colorado State University, 146 pp.

______, 1975: A comparison of the general circulations of the Northern and Southern Hemispheres based on satellite, multi-channel radiance data. Mon Wea. Rev., 103, 52-60.

Benton, G. S. and A. B. Kahn, 1958: Spectra of large-scale atmospheric flow at 300 mb. J. Meteor., 15, 404-410.

Desbois, M., 1975: Large-scale Kinetic energy spectra from eulerian analysis of EOLE wind data. J. Atmos. Sci., 32, 1838-1847.

Kahn, A. B., 1962: Large-scale atmospheric spectra at 200 mb. J. Atmos. Sci., 19, 150-158.

Kao, S. -K. and L. L. Wendell, 1970: The kinetic energy of the large-scale atmospheric motion in wavenumber-frequency space: I. Northern Hemisphere. J. Atmos. Sci., 27, 359-375.

______, R. L. Jenne and J. F. Sagendorf, 1970: The kinetic energy of large-scale atmospheric motion in wavenumber-frequency space: II. Mid-troposphere of the Southern Hemisphere. J. Atmos. Sci., 27, 1000-1020.

Price, P. G., 1975: A comparison between available potential and kinetic energy estimates for the southern and northern hemispheres. Tellus, 27, 443-452.

Saltzman, B., 1958: Some hemispheric spectral statistics. J. Meteor., 15, 259-263.

_______ and A. Fleisher, 1961: Further statistics on the modes of release of available potential energy. J. Geophys. Res., 66, 2271-2273.

_______ and _______, 1962: Spectral statistics of the wind at 500 mb. J. Atmos. Sci., 19, 195-204.

Smith, W. L., H. M. Woolf and W. J. Jacob, 1970: A regression method for obtaining real time temperature and geopotential height profiles from satellite spectrometer measurements and its application to Nimbus III SIRS observations. Mon. Wea. Rev., 98, 582-603.

Taljaard, J. J., H. Van Loon, H. L. Crutcher and R. L. Jenne, 1969: Climate of the Upper Air: Southern Hemisphere. Vol. I, Temperatures, Dew Points and Heights at Selected Pressure Levels. NAVAIR 50-1C-55, Chief of Naval Operations, Washington, D.C., 135 pp.

Van Loon, H., 1972: Wind in the Southern Hemisphere. In Meteorology of the Southern Hemisphere (C. W. Newton, Ed.), Meteor. Monogr., 13, No. 35, 87-100.

Webster, P. J., and D. G. Curtin, 1974: Interpretations of the EOLE Experiment I. Temperal Variation of eulerian quantities. J. Atmos. Sci., 31, 1860-1975.

Wiin-Nielsen, A., 1959: A study of energy conversion and meridional circulation for the large-scale motion in the atmosphere. Mon. Wea. Rev., 87, 319-332.

Wooldridge, G., and E. R. Reiter, 1970: Large-scale atmospheric circulation characteristics as evident from GHOST Balloon Data. <u>J. Atmos. Sci.</u>, 27, 183-194.

Figure Captions

1. Zonal mean geostropic wind at 200 mb in the S.H. for July and January.

2. Spectra of winter 200 mb geostrophic flow at 30° latitude. (a) zonal component, (b) meridional component.

3. Spectra of summer 200 mb geostrophic flow at 30° latitude, (a) zonal component, (b) meridional component.

4. Spectra of winter 200 mb geostrophic flow at 50° latitude. (a) zonal component, (b) meridional component.

5. Anisotropy. Ratio of zonal to meridional spectra coefficients at 200 mb at 50° latitude. (a) winter, (b) summer.

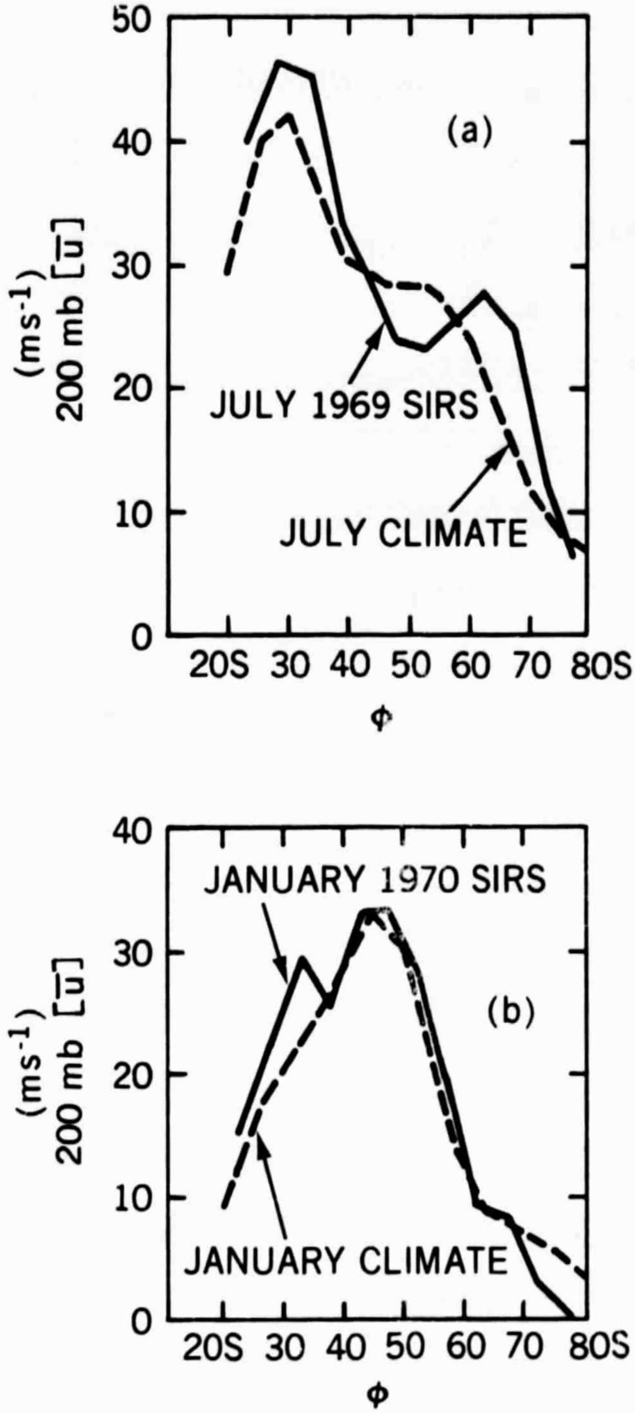

Figure 1. Zonal mean geostropic wind at 200 mb in the S.H. for July and January

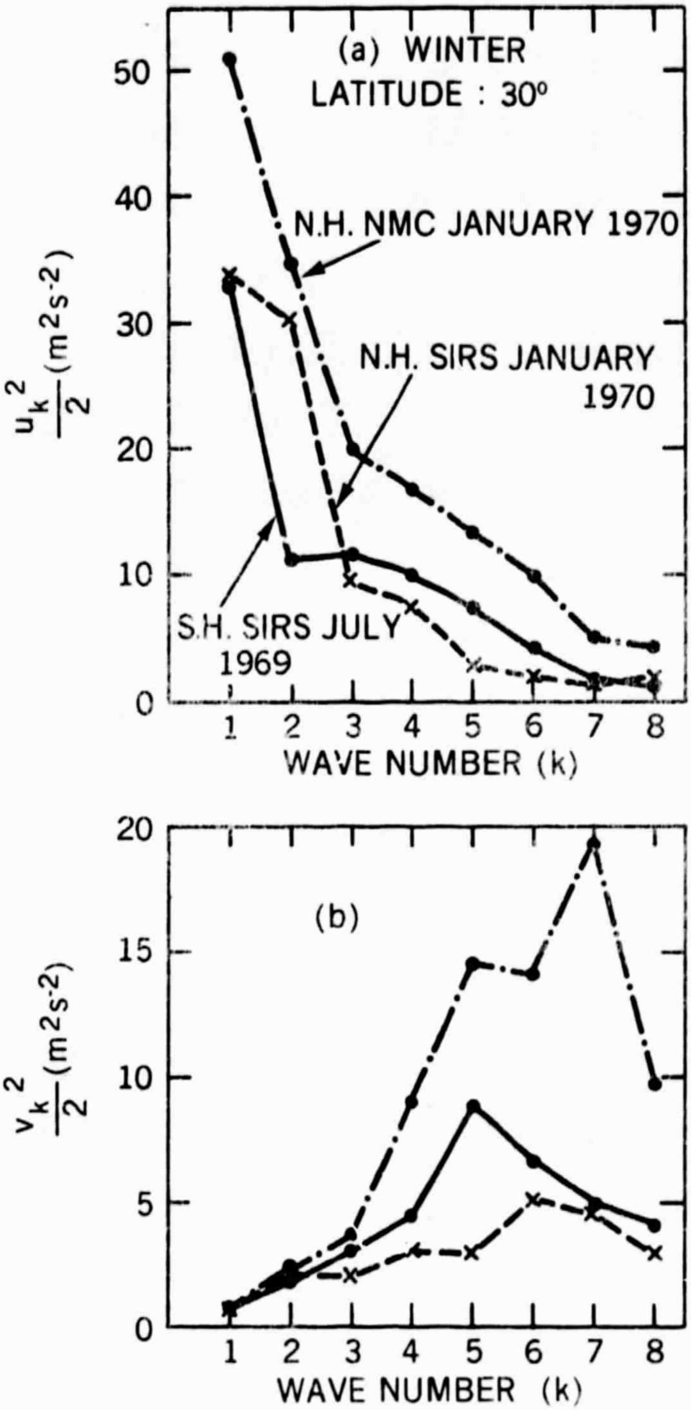

Figure 2. Spectra of winter 200 mb geostrophic flow at 30° latitude. (a) zonal component, (b) meridional component

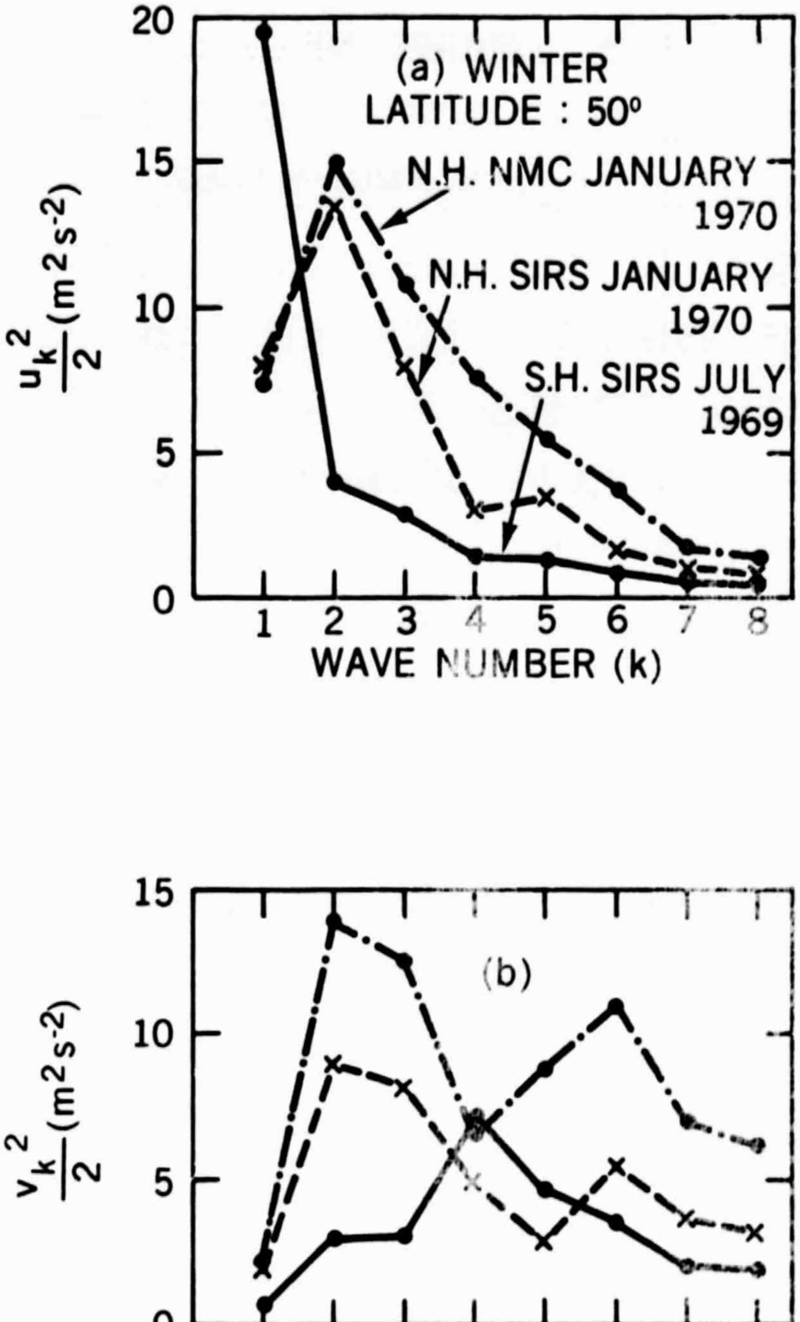

Figure 3. Spectra of summer 200 mb geostrophic flow at 30° latitude, (a) zonal component, (b) meridional component.

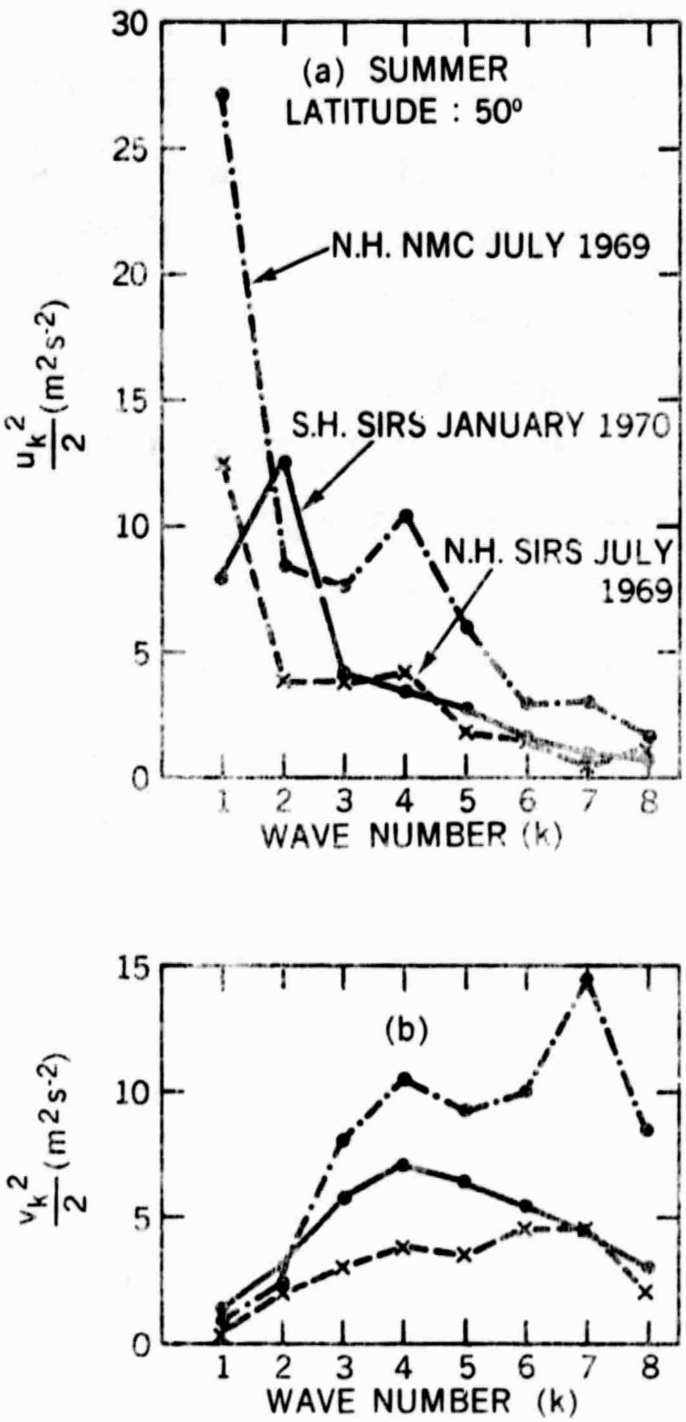

Figure 4. Spectra of winter 200 mb geostrophic flow at 50° latitude. (a) zonal component, (b) meridional component.

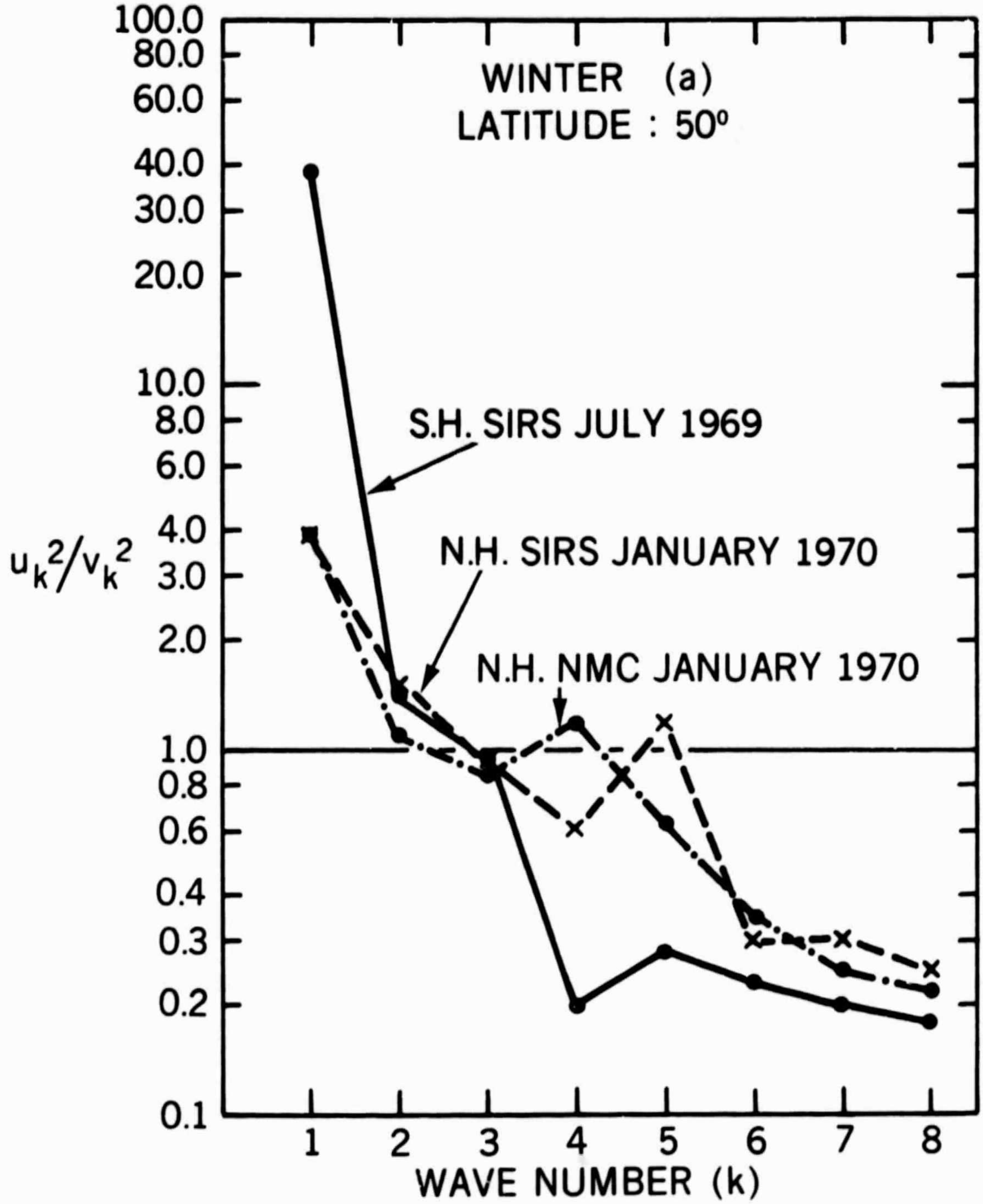

Figure 5a. (Winter) - Anisotropy. Ratio of zonal to meridional spectra coefficients at 200 mb at 50° latitude.

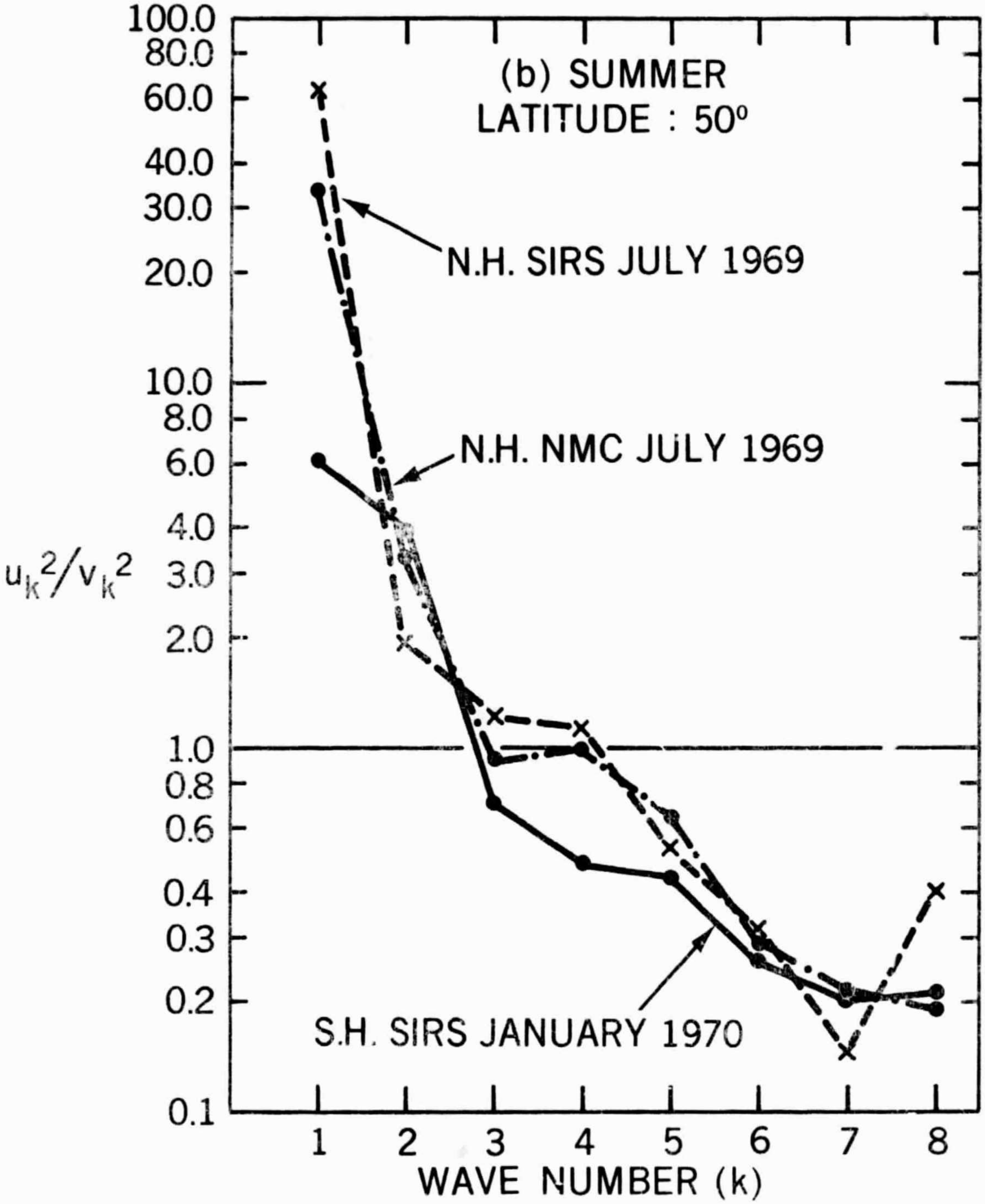

Figure 5b. (Summer) - Anisotropy. Ratio of zonal to meridional spectra coefficients at 200 mb at 50° latitude.